

TADFormer : Task-Adaptive Dynamic TransFormer for Efficient Multi-Task Learning

Seungmin Baek*, Soyul Lee*, Hayeon Jo, Hyesong Choi, Dongbo Min[†]
Ewha Womans University, Korea

{min100kim, 230aig, johayeon, hyesong, dbmin}@ewha.ac.kr

Abstract

Transfer learning paradigm has driven substantial advancements in various vision tasks. However, as state-of-the-art models continue to grow, classical full fine-tuning often becomes computationally impractical, particularly in multi-task learning (MTL) setup where training complexity increases proportional to the number of tasks. Consequently, recent studies have explored Parameter-Efficient Fine-Tuning (PEFT) for MTL architectures. Despite some progress, these approaches still exhibit limitations in capturing fine-grained, task-specific features that are crucial to MTL. In this paper, we introduce **Task-Adaptive Dynamic transFormer**, termed **TADFormer**, a novel PEFT framework that performs task-aware feature adaptation in the fine-grained manner by dynamically considering task-specific input contexts. TADFormer proposes the parameter-efficient prompting for task adaptation and the Dynamic Task Filter (DTF) to capture task information conditioned on input contexts. Experiments on the PASCAL-Context benchmark demonstrate that the proposed method achieves higher accuracy in dense scene understanding tasks, while reducing the number of trainable parameters by up to 8.4 times when compared to full fine-tuning of MTL models. TADFormer also demonstrates superior parameter efficiency and accuracy compared to recent PEFT methods.

1. Introduction

Transfer learning paradigm has achieved significant advancements in the fields of natural language processing [4, 12] and computer vision [18, 48]. Generally, given a pre-trained model on a large-scale dataset, the traditional transfer learning approaches fine-tune an entire model consisting of the pre-trained encoder and task-specific decoder for downstream tasks such as image classification, segmenta-

*These authors contributed equally.

[†]Corresponding author.

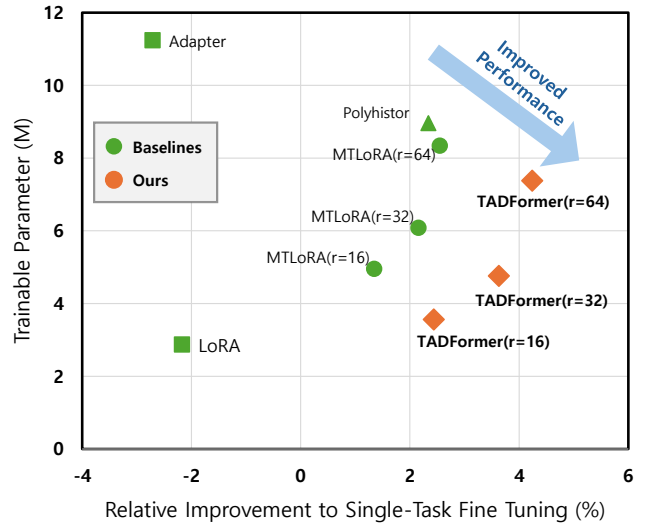


Figure 1. Performance comparison between TADFormer and baseline PEFT methods. Here, r represents the rank of low-rank decomposition modules in both TADFormer and MTLORA.

tion, and object detection. However, as the model capacity of state-of-the-art approaches continue to increase, applying the full fine-tuning to the entire model has become inefficient due to prohibitively high computational resource requirements.

To address this issue, recent works have begun to extensively explore Parameter-Efficient Fine-Tuning (PEFT) [21, 22, 27, 35], which aims to reduce the number of trainable parameters while maintaining the performance on the downstream tasks. For instance, adapter based approaches [20, 21] insert compact modules within Transformer blocks, visual prompt tuning [33, 34] leverages learnable tokens together with inputs or intermediate features, and Low-Rank Adaptation (LoRA) [21] introduces trainable low-rank matrices into Transformer blocks for updating weights.

In a similar context, there have been active attempts to apply the PEFT to Multi-Task Learning (MTL) models [1, 49]. MTL models [3, 23, 50, 52], which aim to simul-

taneously process multiple tasks, generally require more training complexity proportional to the number of tasks, and the PEFT methodologies could be a promising solution to overcome this limitation. Multi-Task LoRA (MTLoRA) [1] extends LoRA [21] to be more suitable for multi-task scenarios, while VMT-adapter [49] implements an MTL architecture based on adapters [20]. Although these methods facilitate parameter-efficient training within MTL models, they still exhibit inherent limitations in terms of leveraging the PEFT in the task-aware manner that fits the MTL architecture.

A primary challenge in training multiple tasks on the single model is to effectively leverage useful information across multiple tasks. To this end, MTL models should effectively capture the unique characteristics of each task while leveraging task-agnostic features by considering interactions between tasks [23, 45]. According to existing MTL studies [52], context information of input samples plays a critical role in enabling the model to capture the unique characteristics of each task. In other words, by considering the diversity of input samples during feature extraction, the model can learn finer-grained, task-specific characteristics. Moreover, when applying PEFT to MTL, only a subset of parameters is fine-tuned, unlike full-tuning, which can limit the model’s adaptability across diverse tasks. This necessitates the approach to extract task-specific features dynamically conditioned on input contexts. However, current PEFT approaches for the MTL model [1, 49] do not reflect sample dependency, extracting task characteristics using only static learnable parameters for each task, which limits their ability to capture task-specific features effectively with only very compact trainable modules.

Moreover, these approaches disregard cross-task relation that is crucial in boosting MTL performance [45, 57]. Fig. 2a conceptually illustrates current PEFT module, which includes both task-shared and task-specific components [1]. This method processes the task-shared and task-specific modules in parallel and do not provide opportunities for task-specific features to interact via task-shared modules.

To overcome these issues, we propose **Task-Adaptive Dynamic transFormer**, termed TADFormer, designed with two objectives; 1) to dynamically extract fine-grained task-specific features while considering interactions between task-specific features, and 2) to design a single module that efficiently extracts the task-specific features. As shown in Fig. 2b, task-adapted features are generated with the help of task attention maps that represent task-specific attributes for each task. They are then fed into a Task-Aware Module (TA-Module) augmented by Dynamic Task Filter (DTF). The DTF adaptively captures fine-grained features by leveraging the context information of input samples through dynamic convolution operations. Furthermore, the distinct

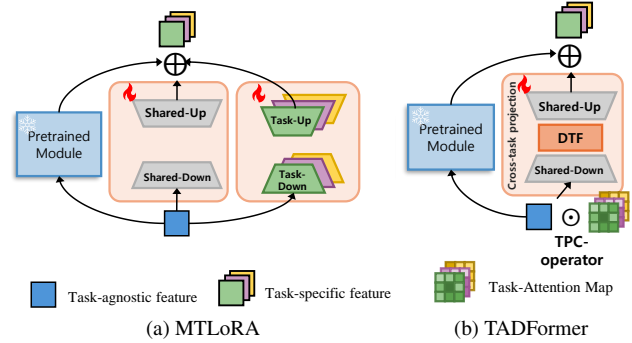


Figure 2. Comparison of MTLoRA [1] and TADFormer. This illustrates the part that extracts and processes task-adapted features. Both methods employ additional trainable down-up projection structures like LoRA [21], in parallel to the frozen pre-trained module. While MTLoRA introduces additional down-up projections for multiple tasks, TADFormer integrates Dynamic Task Filter (DTF), which uses dynamic convolution operations, with minimal additional parameters as well as the TPC-operator using task attention map.

task-adapted features are transmitted through the cross-task projection, which enables the model to consider cross-task relationships. Through the Grad-CAM visualization in Fig. 3, we confirm that our model is capable of extracting fine-grained features more effectively when the input context is considered in the finetuning process.

Our contributions can be summarized as follows:

- We propose TADFormer, a novel PEFT framework for multi-task scene understanding. TADFormer utilizes DTF to dynamically extract task-specific features based on the input context, allowing for more fine-grained task-specific feature learning.
- We propose a prompt-based task adaptation mechanism within the encoder. This approach significantly reduces the number of parameters while effectively learning task-specific features.
- TADFormer achieves higher accuracy while training fewer parameters compared to fully fine-tuning the entire model. TADFormer also demonstrates superior parameter efficiency and accuracy compared to recent PEFT methods as shown in Fig. 1.

2. Related Work

2.1. Multi-Task Learning (MTL)

MTL aims to enable models to learn multiple related tasks simultaneously by sharing information unique to each task [57]. Effective MTL requires capturing useful information in three key areas: task-agnostic representations, task-specific representations, and cross-task interactions. To this end, various MTL approaches have been developed, generally categorized into encoder-focused and decoder-focused

approaches [45]. The encoder-focused architectures primarily facilitate feature sharing within the encoder, using either hard or soft parameter sharing. In the hard parameter sharing strategy, multiple tasks share a common set of parameters in the encoder, while each task has an independent decoder to yield task-specific outputs [2, 28, 41]. In contrast, the soft parameter sharing strategy allows each task to maintain its own set of encoder parameters and exchange cross-task information through modules integrated within the encoder [3, 15]. The decoder-focused architectures [23, 29, 50–52] extend cross-task interactions into the decoding stage. These models typically employ task-specific and cross-task modules within the decoder, enabling tasks to share a single encoder while enabling for more flexible information exchange in the decoders.

2.2. Parameter-Efficient Fine-Tuning (PEFT)

PEFT aims to adapt large-scale pre-trained models [5, 8–10, 13, 19, 30, 30, 31, 31, 37–39, 46, 48, 53] to downstream tasks by tuning only a small subset of parameters, without re-training the entire model. Representative methods include Prompt tuning [33, 34], Adapters [20, 32], and Low-Rank Adaptation (LoRA) [21, 58]. Prompt Tuning introduces trainable tokens to the input of the pre-trained model, facilitating task-specific adaptation without modifying the original weights. Adapters add compact, trainable modules to the model, with only these modules being fine-tuned to adapt the model to specific tasks. AdaptFormer [7] was the first adapter applied to computer vision and demonstrated the effectiveness of adapters in vision tasks by achieving competitive performance. In contrast, LoRA applies low-rank decomposition to the model’s weight matrices, enabling task-specific tuning while maintaining the original weight structure. LoRA is particularly efficient by introducing no additional parameters at inference time as the trainable matrices merge directly with the frozen weights. This allows for effective weight updates with minimal computational overhead. Prompt tuning, Adapters, and LoRA have been successfully applied across various fields of NLP [20, 21, 33] and computer vision [7, 24, 54], demonstrating their versatility and efficiency. Additionally, LoRand [54] introduces multi-branch low-rank adapters to improve performance on dense prediction tasks, and SPT [16] further explores adaptive parameter allocation to task-specific important positions using tuning methods such as LoRA and Adapters.

2.3. PEFT for MTL

MTL experiences increased training complexity due to the proportional growth in decoder size with the number of tasks. To address this, recent research has been actively applying PEFT methods, originally designed for single-task scenarios, to the MTL model. Applying PEFT to multi-task

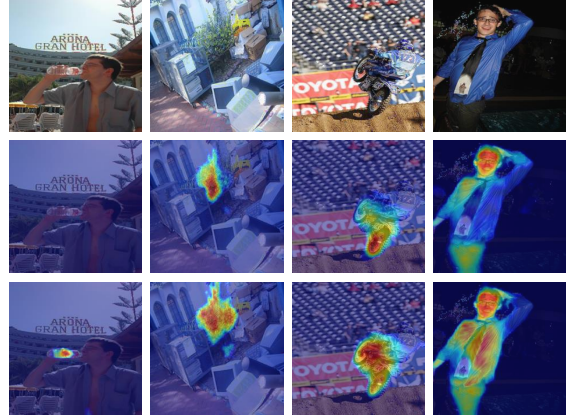


Figure 3. Comparison of Grad-CAM [40] from MTLORA [1] and TADFormer: (from top to bottom) input images, MTLORA, and TADFormer. This demonstrates that TADFormer is capable of extracting fine-grained features that capture the input contexts more precisely, thanks to DTF.

models is challenging in that unique attributes of each task should be extracted through pre-trained models only with small amount of learnable parts. MTLORA [1] and VMT-Adapter [49] have been proposed as PEFT approaches for MTL. MTLORA utilizes LoRA modules consisting of task-agnostic and task-specific components, which effectively separate the parameter space during MTL fine-tuning. In contrast, VMT-Adapter enhances task interactions by sharing knowledge across tasks and preserves task-specific knowledge through independent knowledge extraction modules. However, these approaches struggle to account for the input context when extracting task-specific features, which limits their ability to capture fine-grained details.

3. Method

3.1. Overview

The proposed architecture, TADFormer, consists of a task-shared encoder with a series of Transformer layers and multiple task-specific decoders, as depicted in Fig. 4. A set of task prompts $P = \{p_1^{ini}, \dots, p_T^{ini}\}$ is prepended to image patch tokens $E = \{e_1^{ini}, \dots, e_N^{ini}\}$, forming $X = [P, E]$, and it is then fed into the task-shared Transformer encoder. T and N represent the number of tasks and patch tokens, respectively. Similar to current PEFT approaches for MTL [1], $N - 1$ Transformer blocks of each stage are designed with task-shared modules (TS-Module) consisting of frozen pretrained parts and learnable LoRA modules [21]. In contrast, the last Transformer block, termed Task-Adapting Transformer block in Fig. 4a, is defined with the proposed task-aware modules (TA-Module) that generate task-adaptive and input-dependent features through the task-prompt conditional (TPC) operator and dynamic task

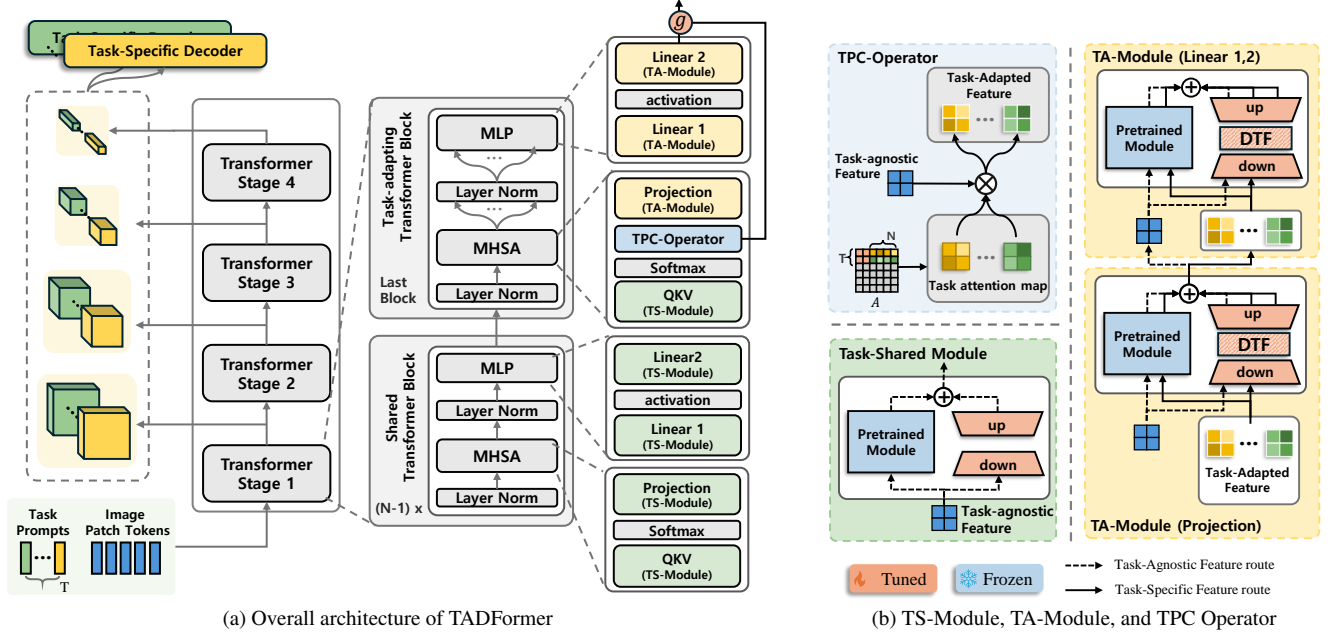


Figure 4. Overview of the proposed TADFormer: (a) The encoder takes as inputs image patch tokens with task prompts prepended. Here, we adopt the VPT shallow approach [24], inserting the task prompts only into the first Transformer stage, and use Swin Transformer [36] as the encoder backbone. In all blocks except the last one of each Transformer stage, the task-agnostic features are extracted through the task-shared module (TS-module). The task-adapting Transformer block extracts fine-grained task-specific features through the task-prompt conditional (TPC) operator and task-aware module (TA-Module), (b) The TPC operator generates the task-adapted features with the help of the task attention map between task prompts and image patch tokens, and these features are then fed into the TA-module consisting of the dynamic task filter (DTF) as well as down-up projections for considering input contexts that are crucial to MTL.

tilter (DTF).

3.2. Task-Shared Module (TS-Module)

To efficiently process task-agnostic feature in a parameter-efficient manner, a frozen pre-trained module $\Phi(\cdot)$ is decomposed into low-rank matrices with down-projection parameters $W_{down} \in \mathbb{R}^{C \times r}$ and up-projection parameters $W_{up} \in \mathbb{R}^{r \times C}$ [21], where $r \ll C$. When an input feature $X_{in} \in \mathbb{R}^{(T+N) \times C}$ is given, a task-agnostic output feature $X_{out} \in \mathbb{R}^{(T+N) \times C}$ from the TS-module is defined as follows:

$$X_{out} = \Phi(X_{in}) + (X_{in}W_{down})W_{up}. \quad (1)$$

Similar to [1] that uses LoRA [21] for efficient tuning in the MTL model, the TS-Module is applied to QKV layer, projection layer, and MLP block within the Transformer blocks, as shown in Fig. 4. Note that while the TS-module is used in all Transformer blocks, the proposed TA-module and TPC operator with the aims of extracting distinct features for tasks are used only in the last Transformer block. This will be detailed in the following sections.

3.3. Task-Prompt Conditional (TPC) Operator

The TPC operator aims to effectively decouple task-specific features from the task-agnostic features, so that the DTF

is capable of extracting representations that further reflects the characteristics of each task. Specifically, it enhances image features of high attention for each task by using task-prompts. Inspired by [10, 51], we propose to use a task attention map between task prompt and patch tokens derived directly from the MHSA module of the Transformer backbone.

3.3.1. Task Attention Map

Task prompts, which are tuned along with task-agnostic feature within the TS-module, are used to extract task-adapted features at the last Transformer block of each stage. In the task-adapting Transformer block of Fig. 4a, the QKV module generates the task-agnostic feature $f_{qkv} \in \mathbb{R}^{N \times C}$ and its associated attention map $A \in \mathbb{R}^{H \times (T+N) \times (T+N)}$, where H is the number of heads in the multi-head self-attention (MHSA). The task attention map $A_{TAM} \in \mathbb{R}^{H \times T \times N}$ between the task prompts and patch tokens is simply obtained from A , such that $A_{TAM} = \{a_1, \dots, a_T\}$ and $a_i \in \mathbb{R}^{H \times 1 \times N}$. Here, a_i indicates how the task prompt p_i relates to all patch tokens $E = \{e_1, \dots, e_N\}$. To match the dimension of the task-agnostic feature to the number of heads, we also reshape f_{qkv} such that $\hat{F} = S(F) \in \mathbb{R}^{H \times C/H \times N}$.

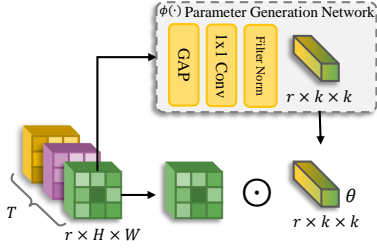


Figure 5. DTF architecture: The down-projected features of channel dimension r are used to generate channel-wise convolution parameters in the parameter generation network. GAP denotes global average pooling.

3.3.2. Task-Adapted Feature

The task-adapted feature $f_i \in \mathbb{R}^{N \times C}$ of the task i for $i = 1, \dots, T$ is computed as follows:

$$f_i = f_{qkv} + S_{\text{inv}}(a_i \otimes \hat{f}_{qkv}), \quad (2)$$

where \otimes is the Hadamard product, and it is repeatedly applied to $\hat{f}_{qkv}(\cdot, k, \cdot)$ for $k = 1, \dots, C/H$. S_{inv} is another reshaping operator, which converts a matrix dimension from $\mathbb{R}^{H \times C/H \times N}$ to $\mathbb{R}^{N \times C}$.

3.4. Task-Aware Module (TA-Module)

The TA-Module is a main component of the TADformer, designed to effectively capture fine-grained task-specific features and perform task-cross interactions. As depicted in Fig. 4b, the TA-module is structured with the Dynamic Task Filter (DTF) inserted between low-rank decomposed parameters used in the TS-Module. The TA-Module processes different inputs depending on its placement within the network. In the projection layer, it processes the task-adapted features, which are outputs of from the TCP-Operator. When applied to the linear layer, it processes the previous TA-module’s output.

3.4.1. Dynamic Task Filter (DTF)

Recent MTL studies [25, 50] emphasize that the contextual information of input instances plays a crucial role in capturing the unique characteristics of each task. Tuning only a subset of parameters to apply PEFT to multi-task models is likely to limit the model’s ability to adapt to multiple tasks and capture task-specific features. To address this challenge, we propose to use the DTF that considers both input and task context within the TA-module, enabling more effective extraction of fine-grained task-specific features. The key objective of DTF is to generate task-customized convolutional parameters $\theta = \{\theta_1, \dots, \theta_T\}$ that reflects the context of the input task-adapted features $f = \{f_1, \dots, f_T\}$ while maintaining trainable parameter-efficiency.

A naive approach for generating task-customized parameters is to directly input the feature f_i into the parameter

generation network $\phi(\cdot)$, such that $\theta_i = \phi(f_i)$. However, it requires processing the entire feature to generate θ , failing to effectively balance trainable parameter efficiency and performance. Instead, we adopt more efficient strategy, in which $\phi(\cdot)$ generates channel-wise convolution parameters θ . Additionally, we apply Global Average Pooling (GAP) to the input features, resulting in a more lightweight network, as depicted in Fig. 5. This approach reduces the number of parameters to $r \times r \times k^2$, where k is the kernel size. The final output \tilde{F} of the TA-module using the DTF is as follows:

$$\theta_i = \phi(f_i W_{\text{down}}) \quad (3)$$

$$\tilde{F}_i = \Phi(f_i) + (\theta_i \odot (f_i W_{\text{down}})) W_{\text{up}} \quad (4)$$

Here, \odot is a channel-wise convolution operations. Additionally, since DTF dynamically adapts to both input and task contexts, training may become unstable, so we employ FilterNorm [59] to the parameter generation network for securing training stability.

3.5. Stage-wise Gating and Skip Connection

The task-wise feature adaptation is conducted through the TPC operator and TS-modules within the block. To further improve usability of the task-adapted feature f_i ($i = 1, \dots, T$) in the task-specific decoders, we introduce the skip connection that adds it to the last Transformer block output \hat{f}_i , which is then fed to the task-specific decoders, as shown in Fig. 4a. This skip connection allows the task-adapted feature f_i , generated through the task prompts in the TPC operator, to be directly passed to the task-specific decoder, allowing the task prompt to better capture attention related to its corresponding task. Additionally, we incorporate a stage-wise gating with a parameter g in the skip connection. A final output of each Transformer stage F_i is as follows:

$$F_i = \sigma(g) \cdot f_i + (1 - \sigma(g)) \cdot \hat{f}_i, \quad (5)$$

where σ indicate the Sigmoid activation function. A trainable gating parameter g is initialized to zero and regulated by the Sigmoid function.

3.6. Selection of Fine-tuning Modules

In the PEFT domain, several studies have been conducted to select which modules are tuned to achieve the best trade-off between downstream task accuracy and efficiency [1, 14]. For example, [1] demonstrated that tuning non-attention modules, such as layer normalization, patch merging layers, and patch embedding layer achieves an effective trade-off in utilizing low-rank adaptation in the hierarchical Transformer baseline, like Swin Transformer [36]. In this regard, we explore an optimal selection of tuning modules in our TADFormer that leverages both low-rank adaptive modules and task-prompt tuning.

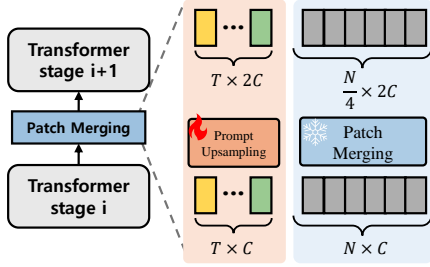


Figure 6. Patch merging module of TADFormer: Leveraging the benefits of task-prompt tuning, we finetune only the prompt upsampling operation that doubles the channel size of the task prompts, while freezing the image patch merging module.

Since our approach is based on the shallow-VPT framework [24] where task prompts are not newly added in the middle of layers, a prompt-upsampling module that doubles the channel size of task prompts is necessary when passing them to the next Transformer stage. Considering the prompt is upsampled in the same position as the patch merging module, we freeze the patch merging module and tune only the prompt upsampling module, as shown in Fig. 6. By tuning only the prompt upsampling module with $2C \times C$ trainable parameters, we achieved competitive performance without additionally tuning the patch merging module with $4C \times 2C$ trainable parameters. Additionally, we tune the layer normalization and positional embedding layers, similar to [1].

4. Experiments

4.1. Implementation Details

Dataset and Evaluation metrics. To evaluate our proposed method, we conducted experiments on the PASCAL-Context dataset, following prior works on PEFT adaptation for MTL [1, 35]. This dataset includes four types of annotations for dense prediction tasks: semantic segmentation with 21 classes, human part segmentation with 7 classes, surface normals estimation, and saliency detection. It consists 4,998 images for training and 5,105 images for testing, respectively. For evaluation, we used the mean intersection-over-union (mIoU) for semantic segmentation, human part segmentation, and saliency detection, and the root mean square error (rmse) for surface normals estimation. Additionally, to assess overall performance across tasks, we measured relative improvement over the single-task fine-tuning baseline as follows:

$$\Delta m = \frac{1}{T} \sum_{i=1}^T (-1)^{l_i} (M_{m,i} - M_{s,i}) / M_{s,i}, \quad (6)$$

where T denotes the number of tasks, $M_{s,i}$ is the single task baseline and $M_{m,i}$ is the performance of the MTL models

on the i -th task. Here, l_i is set to 1 if lower value indicate better performance, otherwise 0.

Implementation. We used the Swin-Transformer pre-trained on the ImageNet dataset [11] as the encoder, and HRNet [42] as the decoder for a fair comparison with existing methods. The decomposed matrices used in TS-Module and TA-Module are configured with ranks of 16, 32, and 64. Also, TS-Module and TA-Module use the same rank size. All experiments were performed in the Pytorch with the same experimental setup as [1]. The experiments in this work are all run on a single NVIDIA V100 GPU environment.

Training. For training the MTL model, we calculated the total loss through weighted sum using weight values corresponding to each task loss as in (7). We used the task weights given in [44].

$$L_{MTL} = \sum_i^T w_i \times L_i \quad (7)$$

where w_i and L_i are the weight and loss of task i . As the loss for each task, standard per-pixel cross-entropy is used for semantic segmentation and human parts segmentation. L1 loss is used for surface normals estimation, and balanced cross-entropy loss is used for saliency detection.

4.2. Baselines

We compared the downstream task accuracy and number of trainable parameters with prior PEFT methods. **Single-task full fine-tuning** is a full fine-tuning model that uses an individual pretrained model for each task. **Adapter** [17] applies task-specific bottleneck modules to each Transformer layer. **Bitfit** [55] tunes only the biases, patch merging layers and patch projection layers. **VPT** [24] tunes the model by prepending a trainable embedding, either to the input (VPT-shallow) or all transformer layers (VPT-deep). **Compacter** [26] decomposes the fast matrix into two low-rank vectors, while **Compacter++** places the modules exclusively after the MLP layers. **LoRA** [21] applies low-rank decomposition to the attention layers, using a rank of 4 and an adapter output scale of 4. **VL-Adapter** [43] simply adds a single adapter to the transformer and shares it across tasks. **Hyperformer** [27] uses a hyper-network that generates adapter weights for different tasks based on task embeddings. **Polyhistor** [35] introduces low-rank hypernetworks and custom kernels to scale fine-tuning parameters across Transformer blocks. **MTLoRA** [1] utilizes a dual-module approach that uses both task-agnostic LoRA modules and task-specific LoRA modules. Task-agnostic LoRA modules capture task-generic features, and task-specific LoRA modules tailor task-specific features from this shared representation.

Table 1. Performance comparison using Swin-T pretrained on ImageNet-1k as the backbone. Here, Δm denotes the relative improvement compared to single-task full fine-tuning. \uparrow and \downarrow indicate whether higher or lower values are preferable, respectively. Bold values indicate that TADFormer yields approximately 1.2-1.7% higher Δm with fewer parameters than MTLORA.

Method	SemSeg ($mIoU \uparrow$)	Human Parts ($mIoU \uparrow$)	Saliency ($mIoU \uparrow$)	Normals ($rmse \downarrow$)	$\Delta m(\%)$	Trainable Parameters (M)
Single Task	67.21	61.93	62.35	17.97	0	112.62
MTL - Tuning Decoders Only	65.09	53.48	57.46	20.69	-9.95	1.94
MTL - Full Fine Tuning	67.56	60.24	65.21	16.64	+2.23	30.06
Adapter [17]	69.21	57.38	61.28	18.83	-2.71	11.24
Bitfit [55]	68.57	55.99	60.64	19.42	-4.60	2.85
VPT-shallow [24]	62.96	52.27	58.31	20.90	-11.18	2.57
VPT-deep [24]	64.35	52.54	58.15	21.07	-10.85	3.43
Compactor [26]	68.08	56.41	60.08	19.22	-4.55	2.78
Compactor++ [26]	67.26	55.69	59.47	19.54	-5.84	2.66
LoRA [21]	70.12	57.73	61.90	18.96	-2.17	2.87
VL-Adapter [43]	70.21	59.15	62.29	19.26	-1.83	4.74
HyperFormer [27]	71.43	60.73	65.54	17.77	+2.64	72.77
Polyhistor [35]	70.87	59.54	65.47	17.47	+2.34	8.96
MTLORA [1] ($r = 16$)	68.19	58.99	64.48	17.03	+1.35	4.95
MTLORA [1] ($r = 32$)	67.74	59.46	64.90	16.59	+2.16	6.08
MTLORA [1] ($r = 64$)	67.9	59.84	65.40	16.60	+2.55	8.34
TADFormer ($r = 16$)	69.79	59.27	65.04	16.91	+2.44	3.56
TADFormer ($r = 32$)	70.2	60	65.71	16.57	+3.63	4.78
TADFormer ($r = 64$)	70.82	60.45	65.88	16.48	+4.24	7.38

Table 2. **Ablation study:** ‘TADFormer Baseline’ refers to the case where all Transformer blocks including the last one utilize only the TS-modules in Fig. 4a. ‘+ TPC-operator + TP’ indicates the performance when the TPC-operator is used with the task prompts (TP) but the DTF is not used. Inversely, ‘+ DTF’ refers to the case that the DTF of the TA-module receives the same features for all tasks, without the TPC-operator and the task prompts. ‘TP + DTF’ includes the DTF and tuning the task prompts, but does not apply TCP-operator using task attention map (TAM) computed from the task prompts.

Method	SemSeg ($mIoU \uparrow$)	Human Parts ($mIoU \uparrow$)	Saliency ($mIoU \uparrow$)	Normals ($rmse \downarrow$)	$\Delta m(\%)$	Trainable Param. (M)
Single Task	67.21	61.93	62.35	17.97	0	112.62
TADFormer Baseline	68.16	59.14	64.72	17.16	+1.3	4.26
+ TPC-operator + TP (A)	68.9 ($\uparrow 0.74$)	59.1 ($\downarrow 0.04$)	64.82 ($\uparrow 0.1$)	17.03 ($\downarrow 0.13$)	+1.79 ($\uparrow 0.49$)	4.66
+ DTF (B)	70.17 ($\uparrow 2.01$)	59.82 ($\uparrow 0.68$)	65.24 ($\uparrow 0.52$)	16.86 ($\downarrow 0.3$)	+2.95 ($\uparrow 1.65$)	4.40
+ TP + DTF	70.29 ($\uparrow 2.13$)	59.8 ($\uparrow 0.66$)	65.5 ($\uparrow 0.78$)	16.75 ($\downarrow 0.41$)	+3.24 ($\uparrow 1.94$)	4.78
TADFormer (A+B)	70.2 ($\uparrow 2.04$)	60 ($\uparrow 0.86$)	65.71 ($\uparrow 0.99$)	16.57 ($\downarrow 0.59$)	+3.63 ($\uparrow 2.33$)	4.78

4.3. Quantitative Analysis

Table 1 shows the MTL performance of all other baseline PEFT methods, including trainable parameters of each methods. For fair comparison, all methods used the Swin-T model [36] pretrained on ImageNet-1k as the backbone. When adapting PEFT to MTL downstream tasks, it is essential to consider 1) the overall multi-task downstream accuracy with 2) the number of trainable parameters relative to the full model parameters. In Table 1, we highlight the results of TADFormer in bold that outperform that the state-of-the-arts [1], while utilizing fewer parameters. These results, reinforced by the structural differences shown in Fig. 2, demonstrate that TADFormer is trained in a more

parameter-efficient manner, making it highly suitable for MTL.

4.4. Ablation Study

The impact of the main modules in TADFormer is reported in the ablation study of Table 2. **1) ‘TADFormer Baseline’** refers to the configuration that utilizes only the TS-modules for all Transformer blocks including the last one, without task-prompt tuning with task prompts prepended to the image patch tokens. **2) ‘+ TPC-operator + TP’** represents the configuration when the ‘TADFormer Baseline’ includes task-prompt tuning (TP) and task-adapting via TCP-operator without using the DTF. **3) ‘+ DTF’** is the model

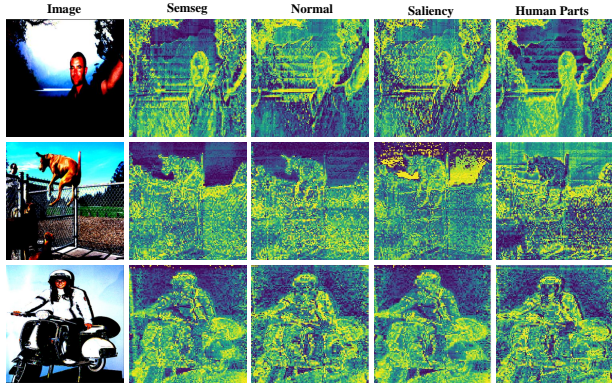


Figure 7. Visualization of the task attention map (TAM) used by the TPC-operator. Notice that the task-prompts corresponding to each task are focused on different parts of the image.

where the DTF is added without the TPC-operator. This model does not include the task prompts as in the TADFormer baseline. **4) '+ TP + DTF'** the DTF and tuning the task prompts (TP), but does not apply TCP-operator using task attention map (TAM) computed from the task prompts. This demonstrate the effectiveness of task attention map (TAM) in TPC-operator to tailor task-adapted features from task-agnostic feature. **5) TADFormer** means our proposed method including all components. The low-rank r is fixed to 32 in all the experiments utilized in Ablation.

Effectiveness of the TPC-operator and DTF. Comparing the performance of 'TADFormer Baseline' and '+ DTF' in Table 2, we can see that the DTF can increase Δm by 1.65. Also, note that '+ DTF' already yields a high performance improvement despite not considering task-context since it does not separate task-adapted features through the TPC. This confirms that the process of extracting input-context sensitive representations via the DTF also is a core component in the MTL performance. Comparing the TADFormer Baseline and '+ TPC operator + TP' in Table 2, we can see an increase in Δm of 0.49. This confirms that the task-adapted feature tailoring process via the task-attention map is significant. The highest Δm performance is achieved by using both TPC-operator with the task prompts and DTF in 'TADFormer'. When the two main components are used together, the TPC-operator passes the task contexts to the DTF. From this, DTF is capable of extracting fine-grained task specific features that take into account both input and task contexts.

Effectiveness of Task Attention Map (TAM) Table 2 also shows the effectiveness of generating task-adapted features by using the TCP-operator based on the task attention map (TAM). 'TADFormer' and '+ TP + DTF' have the same number of trainable parameters, but 0.39 of the Δm is reduced when eliminating the TCP-operator based on the

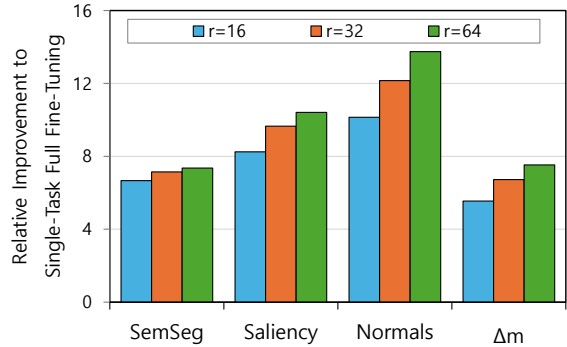


Figure 8. Performance of TADFormer when employing the Swin-Basedel pre-trained on ImageNet-22k.

TAM. This confirms the significance of incorporating task-context features into the model via the TAM. Also, the TAM visualization in Fig. 7 shows that the task prompts are able to capture different regions of attentions for each task.

Analysis on other Backbone and Pre-training Dataset. To verify the applicability of the proposed method to other large backbone models and pre-training datasets, we applied TADFormer to Swin-Base pre-trained on the ImageNet-22k dataset. As shown in Fig. 8, our method demonstrates greater performance improvements when using a larger feature backbone and more pretraining data. This suggests the potential for further performance gains by applying our method to larger model architectures and utilizing additional pretraining data. More experiments are provided in the supplementary material.

Extension to Adapter Baseline. While the proposed method is built upon the LoRA baseline [21], it can also be extended into adapter baselines [7, 49] that are widely adopted recently in PEFT approaches due to low training complexity. These results will be provided in the supplementary material.

5. Conclusion

We have presented a novel PEFT approach that efficiently trains the MTL model for dense scene understanding tasks. To capture fine-grained, task-specific features that are crucial to improving the MTL model, we introduced TPC-operator based on parameter-efficient task prompting and TA-module using the DTF that is capable of reflecting task information conditioned on input contexts. Experiments on four representative tasks, including semantic segmentation, human part segmentation, surface normals estimation, and saliency detection, demonstrate outstanding performance, while keeping training complexity low. Future research includes the extension of this work by leveraging structural knowledge that exists among visual tasks [56].

TADFormer : Task-Adaptive Dynamic TransFormer for Efficient Multi-Task Learning

Supplementary Material

In the supplementary material, we provide more comprehensive results as follows.

- More results using other backbone, pretraining dataset, and decoders
- Analysis on computational efficiency
- TADFormer on adapter-based methods

6. More Results

6.1. TADFormer using other Backbone and Pre-training Dataset

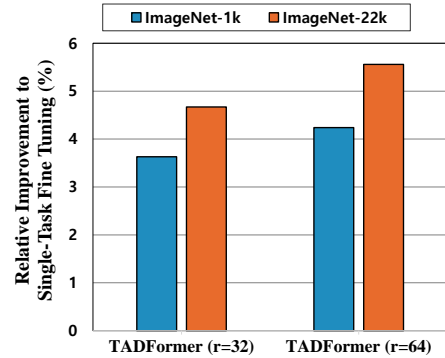
Extending the experiment in Fig. 8, we evaluated the performance of TADFormer using larger pretraining dataset and backbone. As shown in Fig. 9, using the larger pre-training dataset improves performance significantly. Similarly, using the larger backbone, such as Swin-B, also resulted in improved performance. It is worth of noting that the higher relative improvement is achieved when the larger back (Swin-B) or training dataset (ImageNet-22k) are used. These results support the effectiveness of our approach, considering that the performance of single-task fine-tuning, which was used to compute the relative performance improvement, also improves. This demonstrates that TADFormer is the scalable method that can effectively adapt to backbones and pretraining datasets of varying sizes.

6.2. TADFormer using Other Decoders

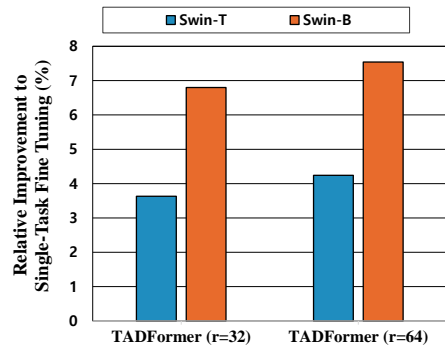
We further evaluated the performance of TADFormer in combination with other decoders. We also compared it with the performance of MTLORA when using the same decoder. Various decoders commonly used in dense prediction tasks were adopted, including HRNet [42], SegFormer [47], and Atrous Spatial Pyramid Pooling (ASPP) [6]. The Swin-T pretrained on ImageNet-22k was used as the encoder. As shown in Table 3, TADFormer demonstrates superior multi-task learning performance with fewer trainable parameters compared to MTLORA across all decoder configurations, confirming that our method is flexible and can be integrated with various decoder architectures. Additionally, ASPP shows the best performance as the decoder with the largest number of trainable parameters, indicating that the choice of decoder enables for an effective trade-off between the performance and the number of trainable parameters.

7. Analysis on Computational Efficiency

Fig. 10 shows the analysis on the computational efficiency in terms of GFLOPs and the number of trainable parameters



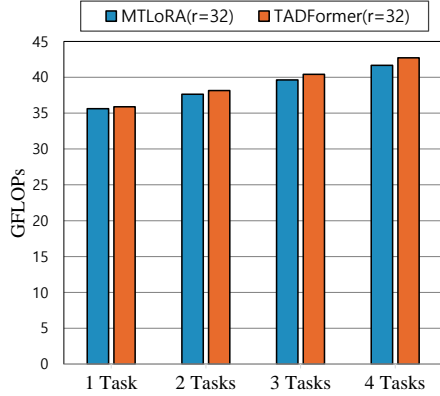
(a) ImageNet-1k vs ImageNet-22k



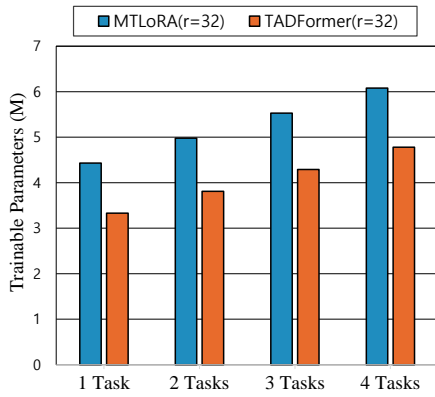
(b) Swin-T vs Swin-B

Figure 9. (a) illustrates the performance difference when using Swin-T pretrained on ImageNet-1k and ImageNet-22k as the backbone of TADFormer. (b) illustrates the performance variation of TADFormer when employing Swin-T and Swin-B, both pretrained on ImageNet-1k.

with respect to the number of tasks. The GFLOPs for both MTLORA and TADFormer are directly measured in this experiment. Compared to MTLORA [1], TADFormer requires slightly more GFLOPs but significantly fewer trainable parameters. This is because the TCP-operator in TADFormer does not require additional parameters, but instead needs additional computation for extracting task-adapted features, and DTF requires additional operations for parameter generation. While TADFormer has a marginal increase in GFLOPs, the substantial reduction in trainable parameters demonstrates its scalability and suitability for efficient multi-task learning scenarios, especially as the number of tasks increases. This trade-off indicates the efficiency of TADFormer in balancing training complexity and parameter optimization.



(a) Comparison of GFLOPs between MTLORA ($r = 32$) and TADFormer ($r = 32$) with respect to the number of tasks.



(b) Comparison of the number of trainable parameters between MTLORA ($r = 32$) and TADFormer ($r = 32$) with respect to the number of tasks.

Figure 10. **Efficiency of TADFormer with different number of tasks:** The experiments were run at the rank $r = 32$.

8. TADFormer on Adapter-Based Methods

Experimental Setup. To analyze the extensibility of TADFormer into other PEFT methods, we experimented TADFormer with adapter-based methods [7, 49]. The comparative analysis is shown in Table 4. The first column (Index) identifies the structures of the modules used in the experiments. The AdaptFormer [7] is the adapter-based PEFT method for single task (**A1**–**A4**). The VMT-Adapter [49] extends the Adapter for MTL in a way that employs the task-shared adapter, similar to AdaptFormer [7], while extracting task-specific features through task-wise scaling and shift operations (**V1**–**V4**). The experiments of the VMT-Adapter were conducted by our implementation, as there is no code available. We also implemented our method on the AdaptFormer (**AO1**–**AO4**) and the VMT-Adapter (**VO1**–**VO4**). ‘seq’ and ‘par’ indicate the sequential and parallel configurations of the adapter with MLP module as shown in Fig. 11. Please refer to the caption of Table 4 for more details on ρ and r .

An example of applying our method, TADFormer, to the AdaptFormer [7] is described in Fig. 12 (**AO2** or **AO4**). This design allows the TADFormer module to be integrated into adapter-based PEFT methods, taking into account both task and input contexts. This architecture can be applied to both parallel and sequential configuration of adapters and is equally applicable to other adapter-based method such as VMT-Adapter [49].

In the following, we compared the existing adapter-based methods [7, 49] with our method implemented on the adapter framework. For a fair comparison, we evaluated the performance for the cases with the similar amount of trainable parameters, though the results of all possible combinations are provided in Table 4. Our code on the adapter-based experiments is submitted as supplementary material.

AdaptFormer vs. AdaptFormer with Ours. For a fair comparison in terms of the number of trainable parameters, we compared **A1**, **A2** and **AO3**, **AO4** that have comparable numbers of trainable parameters. In both comparison, TADFormer demonstrated higher Δm values when integrated into both sequential and parallel configurations. This reveals that the application of TADFormer to AdaptFormer results in an overall enhancement in MTL performance.

VMT-Adapter vs. AdaptFormer with Ours. As the VMT-Adapter [49] is an extension of the AdaptFormer [7], we applied our method to the AdaptFormer, and then compared it with VMT-Adapter. To be specific, the model proposed in [49] uses the down-projection ratio of $\rho = 4$ (**V2**). For a fair comparison in terms of the number of trainable parameters, we compared it with the AdaptFormer combined with TADFormer using $r = 64$ (**AO4**). This makes their number of parameters comparable. In comparison, **AO4** achieves a Δm increase of 4.07 with only an additional 0.02 M trainable parameters compared to **V2**. The comparison of **V1** and **AO3** also shows a similar tendency. This result demonstrates that the structure of TADFormer is more effective for multi-task learning than the scaling and shift operations used in the VMT-Adapter.

VMT-Adapter vs. VMT-Adapter with Ours. We also compared **V1**, **V2** with **VO3**, **VO4**, which have comparable numbers of trainable parameters, demonstrating that the performance has notably improved with only 0.3M increase in trainable parameters. This suggests that even when the adapter’s down-projection channel dimension is reduced to reduce trainable parameters, the structure of TADFormer is capable of efficiently and effectively extracting multi-task representations.

To sum up, these results confirm that the TADFormer can be successfully integrated into various adapter-based methods and is the scalable multi-task PEFT method, compatible with both LoRA and adapter-based frameworks.

Table 3. **Performance comparison with other decoders:** For the encoder, we use TADFormer ($r = 32$) and MTLORA ($r = 32$) with the Swin-T backbone pretrained on ImageNet-22k.

Method	Model Encoder	Decoder	SemSeg ($mIoU \uparrow$)	Human Parts ($mIoU \uparrow$)	Saliency ($mIoU \uparrow$)	Normals ($rmse \downarrow$)	$\Delta m(\%)$	Trainable Param. (M) Decoder / All
MTLORA [1]	Swin-T	HRNet [42]	69.44	61.08	63.24	16.47	+2.93	1.94 / 6.08
		SegFormer [47]	69.59	61.13	63.74	16.62	+3.00	2.08 / 6.22
		ASPP [6]	72.32	60.98	63.04	16.51	+3.83	12.44 / 16.58
TADFormer	Swin-T	HRNet [42]	72.05	61.6	65.45	16.7	+4.67	1.94 / 4.78
		SegFormer [47]	72.33	61.16	65.8	16.87	+4.51	2.08 / 4.91
		ASPP [6]	73.66	60.37	65.27	16.43	+5.09	12.44 / 15.27

Table 4. **Performance comparison with Adapter-based PEFT Methods:** In the adapter-based PEFT, the input feature is down-projected and up-projected within the adapter ($d \rightarrow r \rightarrow d$), where d is the dimension of an input feature and r is the dimension of hidden layer, which is also called rank. In our experiments, we consider two types of projection dimensions: 1) $\rho = \frac{d}{r}$ denotes the down-projection ratio used in the adapter, 2) $r = 64$ denotes a fixed down-projected channel dimension. Additionally, ‘seq’ and ‘par’ indicate the sequential and parallel configurations of the adapter with MLP module as shown in Fig. 11. This experiment demonstrates the performance of integrating TADFormer with two adapter-based PEFT methods: AdaptFormer and VMT-Adapter. AdaptFormer uses a shared adapter structure for all tasks. VMT-Adapter, similar to AdaptFormer, utilizes a shared adapter but additionally incorporates task-specific scaling and shift operations. * indicates that the results were reproduced by our implementation, as there is no code available. All results were obtained using the Swin-T pre-trained on ImageNet-1k as in Table 1.

Index	Method	SemSeg ($mIoU \uparrow$)	Human Parts ($mIoU \uparrow$)	Saliency ($mIoU \uparrow$)	Normals ($rmse \downarrow$)	$\Delta m(\%)$	Trainable Parameters (M)
S	Single Task	67.21	61.93	62.35	17.97	0	112.62
M1	MTL - Tuning Decoders Only	65.09	53.48	57.46	20.69	-9.95	1.94
M2	MTL - Full Fine Tuning	67.56	60.24	65.21	16.64	+2.23	30.06
A1	AdaptFormer (seq) [7] ($\rho = 4$)	69.01	58.2031	63.545	18.1676	-0.63	3.64
A2	AdaptFormer (par) [7] ($\rho = 4$)	55.28	50.63	60.51	18.55	-10.54	3.64
A3	AdaptFormer (seq) [7] ($r = 64$)	68.84	57.84	63.57	18.46	-1.23	3.12
A4	AdaptFormer (par) [7] ($r = 64$)	55.18	50.39	60.36	18.78	-11.06	3.12
AO1	AdaptFormer+Ours (seq) ($\rho = 4$)	72	59.62	64.94	17.4	2.69	4.48
AO2	AdaptFormer+Ours (par) ($\rho = 4$)	61.41	52.93	62.88	17.57	-5.02	4.48
AO3	AdaptFormer+Ours (seq) ($r = 64$)	71.74	58.56	64.38	17.52	1.76	3.67
AO4	AdaptFormer+Ours (par) ($r = 64$)	60.37	52.18	62.46	17.83	-6.25	3.67
V1	VMT-Adapter (seq)* [49] ($\rho = 4$)	68.98	58.44	63.43	18.26	-0.71	3.65
V2	VMT-Adapter (par)* [49] ($\rho = 4$)	55.4	50.98	60.45	18.5	-10.32	3.65
V3	VMT-Adapter (seq)* [49] ($r = 64$)	68.8	58	63.59	18.42	-1.12	3.14
V4	VMT-Adapter (par)* [49] ($r = 64$)	55.25	50.32	60.38	18.76	-11.03	3.14
VO1	VMT-Adapter+Ours (seq) ($\rho = 4$)	71.91	59.6	64.7	17.37	+2.59	4.49
VO2	VMT-Adapter+Ours (par) ($\rho = 4$)	60.89	52.59	62.58	17.57	-5.48	4.49
VO3	VMT-Adapter+Ours (seq) ($r = 64$)	71.7	58.72	64.64	17.57	+1.85	3.68
VO4	VMT-Adapter+Ours (par) ($r = 64$)	59.81	51.55	62.3	17.9	-6.87	3.68

References

- [1] Ahmed Agiza, Marina Neseem, and Sherief Reda. Mtlora: Low-rank adaptation approach for efficient multi-task learning. In *Proceedings of the IEEE/CVF Conference on Computer Vision and Pattern Recognition*, pages 16196–16205, 2024. 1, 2, 3, 4, 5, 6, 7
- [2] Giannis Bekoulis, Johannes Deleu, Thomas Demeester, and Chris Develder. Adversarial training for multi-context joint entity and relation extraction. *arXiv preprint arXiv:1808.06876*, 2018. 3
- [3] Deblina Bhattacharjee, Tong Zhang, Sabine Süsstrunk, and Mathieu Salzmann. Mult: An end-to-end multitask learning transformer. In *Proceedings of the IEEE/CVF Conference on Computer Vision and Pattern Recognition*, pages 12031–12041, 2022. 1, 3
- [4] Tom Brown, Benjamin Mann, Nick Ryder, Melanie Subbiah, Jared D. Kaplan, Prafulla Dhariwal, Arvind Neelakantan, Pranav Shyam, Girish Sastry, Amanda Askell, et al. Language models are few-shot learners. In *Advances in Neural Information Processing Systems*, 2020. 1
- [5] Nicolas Carion, Francisco Massa, Gabriel Synnaeve, Nicolas Usunier, Alexander Kirillov, and Sergey Zagoruyko. End-to-end object detection with transformers. In *European conference on computer vision*, pages 213–229. Springer, 2020. 3
- [6] Liang-Chieh Chen, Yukun Zhu, George Papandreou, Florian

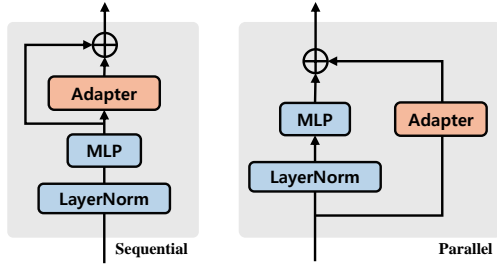


Figure 11. Adapter configuration: Both sequential and parallel configurations are possible in adapter-based PEFT framework [7].

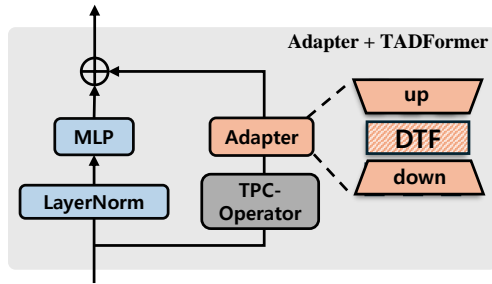


Figure 12. Overview of Adapter + TADFormer in parallel adapter configuration

Schroff, and Hartwig Adam. Encoder-decoder with atrous separable convolution for semantic image segmentation. In *Proceedings of the European conference on computer vision (ECCV)*, pages 801–818, 2018. 1, 3

- [7] Shijie Chen, Chongjian Ge, Zhanhong Tong, Jianmin Wang, Yang Song, Jianbo Wang, and Ping Luo. Adaptformer: Adapting vision transformers for scalable visual recognition. In *Advances in Neural Information Processing Systems*, pages 16664–16678, 2022. 3, 8, 2, 4
- [8] Hyesong Choi, Daeun Kim, Sungmin Cha, Kwang Moo Yi, and Dongbo Min. Improving generative pre-training: An in-depth study of masked image modeling and denoising models. *arXiv preprint arXiv:2412.19104*, 2024. 3
- [9] Hyesong Choi, Hunsang Lee, Seyoung Joung, Hyejin Park, Jiyeong Kim, and Dongbo Min. Emerging property of masked token for effective pre-training. *arXiv preprint arXiv:2404.08330*, 2024.
- [10] Hyesong Choi, Hyejin Park, Kwang Moo Yi, Sungmin Cha, and Dongbo Min. Saliency-based adaptive masking: revisiting token dynamics for enhanced pre-training. In *European Conference on Computer Vision*, pages 343–359. Springer, 2025. 3, 4
- [11] Jia Deng, Wei Dong, Richard Socher, Li-Jia Li, Kai Li, and Li Fei-Fei. Imagenet: A large-scale hierarchical image database. In *2009 IEEE conference on computer vision and pattern recognition*, pages 248–255. Ieee, 2009. 6
- [12] Jacob Devlin, Ming-Wei Chang, Kenton Lee, and Kristina Toutanova. Bert: Pre-training of deep bidirectional transformers for language understanding. In *Proceedings of the Annual Conference of the North American Chapter of the Association for Computational Linguistics*, 2018. 1
- [13] Alexey Dosovitskiy, Lucas Beyer, Alexander Kolesnikov, Dirk Weissenborn, Xiaohua Zhai, Thomas Unterthiner, Mostafa Dehghani, Matthias Minderer, Georg Heigold, Sylvain Gelly, Jakob Uszkoreit, and Neil Houlsby. An image is worth 16x16 words: Transformers for image recognition at scale, 2021. 3
- [14] Peng Gao, Jiaming Han, Renrui Zhang, Ziyi Lin, Shijie Geng, Aojun Zhou, Wei Zhang, Pan Lu, Conghui He, Xiangyu Yue, et al. Llama-adapter v2: Parameter-efficient visual instruction model. *arXiv preprint arXiv:2304.15010*, 2023. 5
- [15] Yihang Gao, Jun Ma, Mingbo Zhao, Wei Liu, and Alan L. Yuille. Nddr-cnn: Layerwise feature fusing in multi-task cnns by neural discriminative dimensionality reduction. In *Proceedings of the IEEE/CVF Conference on Computer Vision and Pattern Recognition (CVPR)*, 2019. 3
- [16] Haotao He, Jianfei Cai, Jing Zhang, Dacheng Tao, and Bohan Zhuang. Sensitivity-aware visual parameter-efficient fine-tuning. In *Proceedings of the IEEE/CVF International Conference on Computer Vision*, pages 11825–11835, 2023. 3
- [17] Junxian He, Chunting Zhou, Xuezhe Ma, Taylor Berg-Kirkpatrick, and Graham Neubig. Towards a unified view of parameter-efficient transfer learning. *arXiv preprint arXiv:2110.04366*, 2021. 6, 7
- [18] Kaiming He, Xinlei Chen, Saining Xie, Yanghao Li, Piotr Dollár, and Ross Girshick. Masked autoencoders are scalable vision learners. In *Proceedings of the IEEE Conference on Computer Vision and Pattern Recognition*, 2022. 1
- [19] Kaiming He, Xinlei Chen, Saining Xie, Yanghao Li, Piotr Dollár, and Ross Girshick. Masked autoencoders are scalable vision learners. In *Proceedings of the IEEE/CVF conference on computer vision and pattern recognition*, pages 16000–16009, 2022. 3
- [20] Neil Houlsby, Andrei Giurgiu, Stanislaw Jastrzebski, Bruna Morrone, Quentin De Laroussilhe, Andrea Gesmundo, Mona Attariyan, and Sylvain Gelly. Parameter-efficient transfer learning for nlp. In *International Conference on Machine Learning*, pages 2790–2799. PMLR, 2019. 1, 2, 3
- [21] Edward J. Hu et al. Lora: Low-rank adaptation of large language models. *arXiv preprint arXiv:2106.09685*, 2021. 1, 2, 3, 4, 6, 7, 8
- [22] Zhiqiang Hu, Yihuai Lan, Lei Wang, Wanyu Xu, Eepeng Lim, Roy Ka-Wei Lee, Lidong Bing, and Soujanya Poria. Llm-adapters: An adapter family for parameter-efficient fine-tuning of large language models. *arXiv preprint arXiv:2304.01933*, 2023. 1
- [23] Huimin Huang et al. Going beyond multi-task dense prediction with synergy embedding models. In *Proceedings of the IEEE/CVF Conference on Computer Vision and Pattern Recognition*, page to appear, 2024. 1, 2, 3
- [24] Menglin Jia, Luming Tang, Bor-Chun Chen, Claire Cardie, Serge Belongie, Bharath Hariharan, and Ser-Nam Lim. Visual prompt tuning. In *European Conference on Computer Vision*, pages 709–727. Springer, 2022. 3, 4, 6, 7

- [25] Xu Jia, Bert De Brabandere, Tinne Tuytelaars, and Luc V Gool. Dynamic filter networks. *Advances in neural information processing systems*, 29, 2016. 5
- [26] Rabeeh Karimi Mahabadi, James Henderson, and Sebastian Ruder. Compacter: Efficient low-rank hypercomplex adapter layers. In *Advances in Neural Information Processing Systems*, pages 1022–1035, 2021. 6, 7
- [27] Rabeeh Karimi Mahabadi, Sebastian Ruder, Mostafa Dehghani, and James Henderson. Parameter-efficient multi-task fine-tuning for transformers via shared hypernetworks. *arXiv preprint arXiv:2106.04489*, 2021. 1, 6, 7
- [28] Alex Kendall, Yarin Gal, and Roberto Cipolla. Multi-task learning using uncertainty to weigh losses for scene geometry and semantics. In *Proceedings of the IEEE Conference on Computer Vision and Pattern Recognition*, pages 7482–7491, 2018. 3
- [29] Sunkyoung Kim, Hyesong Choi, and Dongbo Min. Sequential cross attention based multi-task learning. In *2022 IEEE International Conference on Image Processing (ICIP)*, pages 2311–2315. IEEE, 2022. 3
- [30] Hunsang Lee, Hyesong Choi, Kwanghoon Sohn, and Dongbo Min. Knn local attention for image restoration. In *Proceedings of the IEEE/CVF conference on computer vision and pattern recognition*, pages 2139–2149, 2022. 3
- [31] Hunsang Lee, Hyesong Choi, Kwanghoon Sohn, and Dongbo Min. Cross-scale knn image transformer for image restoration. *IEEE Access*, 11:13013–13027, 2023. 3
- [32] Tao Lei, Junlin Bai, Siddhartha Brahma, Joshua Ainslie, Kenton Lee, Yi Zhou, Ming-Wei Chang, et al. Conditional adapters: Parameter-efficient transfer learning with fast inference. In *Advances in Neural Information Processing Systems*, pages 8152–8172, 2023. 3
- [33] Brian Lester, Rami Al-Rfou, and Noah Constant. The power of scale for parameter-efficient prompt tuning. *arXiv preprint arXiv:2104.08691*, 2021. 1, 3
- [34] Xiang Lisa Li and Percy Liang. Prefix-tuning: Optimizing continuous prompts for generation. *arXiv preprint arXiv:2101.00190*, 2021. 1, 3
- [35] Yen-Cheng Liu, Chih-Yao Ma, Junjiao Tian, Zijian He, and Zsolt Kira. Polyhistor: Parameter-efficient multi-task adaptation for dense vision tasks. In *Advances in Neural Information Processing Systems*, pages 36889–36901, 2022. 1, 6, 7
- [36] Ze Liu, Yutong Lin, Yue Cao, Han Hu, Yixuan Wei, Zheng Zhang, Stephen Lin, and Baining Guo. Swin transformer: Hierarchical vision transformer using shifted windows. In *Proceedings of the IEEE/CVF international conference on computer vision*, pages 10012–10022, 2021. 4, 5, 7
- [37] Ze Liu, Yutong Lin, Yue Cao, Han Hu, Yixuan Wei, Zheng Zhang, Stephen Lin, and Baining Guo. Swin transformer: Hierarchical vision transformer using shifted windows, 2021. 3
- [38] Ze Liu, Han Hu, Yutong Lin, Zhuliang Yao, Zhenda Xie, Yixuan Wei, Jia Ning, Yue Cao, Zheng Zhang, Li Dong, et al. Swin transformer v2: Scaling up capacity and resolution. In *Proceedings of the IEEE/CVF conference on computer vision and pattern recognition*, pages 12009–12019, 2022.
- [39] René Ranftl, Alexey Bochkovskiy, and Vladlen Koltun. Vision transformers for dense prediction. In *Proceedings of the IEEE/CVF international conference on computer vision*, pages 12179–12188, 2021. 3
- [40] Ramprasaath R Selvaraju, Michael Cogswell, Abhishek Das, Ramakrishna Vedantam, Devi Parikh, and Dhruv Batra. Grad-cam: Visual explanations from deep networks via gradient-based localization. In *Proceedings of the IEEE international conference on computer vision*, pages 618–626, 2017. 3
- [41] Ozan Sener and Vladlen Koltun. Multi-task learning as multi-objective optimization. In *Advances in Neural Information Processing Systems*, 2018. 3
- [42] Ke Sun, Bin Xiao, Dong Liu, and Jingdong Wang. Deep high-resolution representation learning for human pose estimation. In *Proceedings of the IEEE/CVF conference on computer vision and pattern recognition*, pages 5693–5703, 2019. 6, 1, 3
- [43] Yi-Lin Sung, Jaemin Cho, and Mohit Bansal. VL-Adapter: Parameter-efficient transfer learning for vision-and-language tasks. In *Proceedings of the IEEE/CVF Conference on Computer Vision and Pattern Recognition*, pages 5227–5237, 2022. 6, 7
- [44] Simon Vandenhende, Stamatios Georgoulis, and Luc Van Gool. Mti-net: Multi-scale task interaction networks for multi-task learning. In *Computer Vision—ECCV 2020: 16th European Conference, Glasgow, UK, August 23–28, 2020, Proceedings, Part IV 16*, pages 527–543. Springer, 2020. 6
- [45] Simon Vandenhende, Stamatios Georgoulis, Wouter Van Gansbeke, Marc Proesmans, Dengxin Dai, and Luc Van Gool. Multi-task learning for dense prediction tasks: A survey. *IEEE transactions on pattern analysis and machine intelligence*, 44(7):3614–3633, 2021. 2, 3
- [46] Enze Xie, Wenhai Wang, Zhiding Yu, Anima Anandkumar, Jose M Alvarez, and Ping Luo. Segformer: Simple and efficient design for semantic segmentation with transformers. *Advances in neural information processing systems*, 34: 12077–12090, 2021. 3
- [47] Enze Xie, Wenhai Wang, Zhiding Yu, Anima Anandkumar, Jose M Alvarez, and Ping Luo. Segformer: Simple and efficient design for semantic segmentation with transformers. *Advances in neural information processing systems*, 34: 12077–12090, 2021. 1, 3
- [48] Zhenda Xie, Zheng Zhang, Yue Cao, Yutong Lin, Jianmin Bao, Zhuliang Yao, Qi Dai, and Han Hu. Simmim: A simple framework for masked image modeling. In *Proceedings of the IEEE/CVF Conference on Computer Vision and Pattern Recognition*, 2022. 1, 3
- [49] Yi Xin, Junlong Du, Qiang Wang, Zhiwen Lin, and Ke Yan. Vmt-adapter: Parameter-efficient transfer learning for multi-task dense scene understanding. In *Proceedings of the AAAI Conference on Artificial Intelligence*, pages 16085–16093, 2024. 1, 2, 3, 8
- [50] Yutong Yang, Peng-Tao Jiang, Qibin Hou, Hao Zhang, Jinhui Chen, and Bing Li. Multi-task dense prediction via mixture of low-rank experts. In *Proceedings of the IEEE/CVF Conference on Computer Vision and Pattern Recognition*, pages 27927–27937, 2024. 1, 3, 5

- [51] Hanrong Ye and Dan Xu. Taskprompter: Spatial-channel multi-task prompting for dense scene understanding. In *The Eleventh International Conference on Learning Representations*, 2022. [4](#)
- [52] Hanrong Ye and Dan Xu. Taskexpert: Dynamically assembling multi-task representations with memorial mixture-of-experts. In *Proceedings of the IEEE/CVF International Conference on Computer Vision*, 2023. [1](#), [2](#), [3](#)
- [53] Kun Yi, Yixiao Ge, Xiaotong Li, Shusheng Yang, Dian Li, Jianping Wu, Ying Shan, and Xiaohu Qie. Masked image modeling with denoising contrast. *arXiv preprint arXiv:2205.09616*, 2022. [3](#)
- [54] Dongqi Yin, Yi Yang, Zilong Wang, Hao Yu, Ke Wei, and Xia Sun. 1% vs 100%: Parameter-efficient low rank adapter for dense predictions. In *Proceedings of the IEEE/CVF Conference on Computer Vision and Pattern Recognition*, pages 20116–20126, 2023. [3](#)
- [55] Elad Ben Zaken, Shauli Ravfogel, and Yoav Goldberg. Bitfit: Simple parameter-efficient fine-tuning for transformer-based masked language models. *arXiv preprint arXiv:2106.10199*, 2021. [6](#), [7](#)
- [56] Amir R. Zamir, Alexander Sax, William Shen, Leonidas J. Guibas, Jitendra Malik, and Silvio Savarese. Taskonomy: Disentangling task transfer learning. In *Proceedings of the IEEE Conference on Computer Vision and Pattern Recognition (CVPR)*, 2018. [8](#)
- [57] Yu Zhang and Qiang Yang. A survey on multi-task learning. *IEEE transactions on knowledge and data engineering*, 34(12):5586–5609, 2021. [2](#)
- [58] Zihan Zhong, Zhiqiang Tang, Tong He, Haoyang Fang, and Chun Yuan. Convolution meets lora: Parameter efficient finetuning for segment anything model. In *Proceedings of the International Conference on Learning Representations*, 2024. [3](#)
- [59] Jingkai Zhou, Varun Jampani, Zhixiong Pi, Qiong Liu, and Ming-Hsuan Yang. Decoupled dynamic filter networks. In *Proceedings of the IEEE/CVF Conference on Computer Vision and Pattern Recognition*, pages 6647–6656, 2021. [5](#)